

## Conformation-Dependent Binding of Diheptanoylphosphatidylcholine by Cyclodextrins As Revealed by Proton Nuclear Magnetic Resonance

Seiji Ishikawa, Saburo Neya, and Noriaki Funasaki\*

Kyoto Pharmaceutical University, Misasagi, Yamashina-ku, Kyoto 607-8414, Japan

Received: September 5, 1997; In Final Form: January 22, 1998

The complex formation of 1 mmol kg<sup>-1</sup> diheptanoylphosphatidylcholine (DHPC) with  $\alpha$ - and  $\gamma$ -cyclodextrins (CD) in deuterium oxide solutions has been investigated by proton nuclear magnetic resonance. With the addition of CD, the variations in proton chemical shifts of DHPC and in vicinal coupling constants of the glycerol C1H<sub>2</sub>–C2H protons allow us to estimate the equilibrium constant and stoichiometry of complexation and to image the three-dimensional structures of their complexes. The addition of  $\alpha$ -CD causes an increase of the trans conformer (T) of DHPC and a decrease of the gauche<sup>+</sup> conformer (G<sup>+</sup>), whereas the addition of  $\gamma$ -CD results in the reverse changes. From the dependence of the chemical shift of a DHPC proton on the CD concentration, we estimate the equilibrium formation macroconstants  $K_1$  and  $K_2$  of 1:1 and 1:2 complexations of DHPC and CD. In contrast with the case for single-chain surfactants, the  $K_1$  value for  $\alpha$ -CD is smaller than that for  $\gamma$ -CD and the  $K_2$  value for  $\gamma$ -CD is smaller than  $K_1$  for  $\gamma$ -CD. The equilibrium microconstants of CD complexation of the three rotamers G<sup>+</sup>, G<sup>-</sup> (gauche<sup>-</sup>), and T of DHPC are also estimated from the concentration dependence of vicinal coupling constants. Predominant binary complexes of  $\alpha$ -CD and  $\gamma$ -CD are composed of the G<sup>-</sup> form and the G<sup>+</sup> form, respectively. The T of the three conformers of DHPC tends most easily to form the ternary complex with  $\alpha$ -CD and  $\gamma$ -CD. There seems to be almost no distinction between the 1- and 2-heptanoyl chains of DHPC for binding to the  $\alpha$ -CD cavity. The inclusion of DHPC into the  $\gamma$ -CD cavity induces magnetic nonequivalence of the terminal methyl protons of chains 1 and 2. It is likely that DHPC is bound from the side of secondary hydroxyl groups of  $\gamma$ -CD. The three-dimensional structures of major complexes are proposed on the basis of the magnitude of chemical-shift variation of each proton of DHPC and CD. The intermediate methylene groups of DHPC are located near the center of an  $\alpha$ -CD cavity, whereas the two terminal methyl groups of DHPC are deeply penetrated into a  $\gamma$ -CD cavity. The above results are discussed in relation to the hemolysis of erythrocytes, one of the serious toxicities of CD caused when it was added in foods and pharmaceuticals.

### Introduction

Cyclodextrins have homogeneous toroidal structures of different molecular sizes. For instance,  $\beta$ -cyclodextrin contains 7 glucose units and 35 stereogenic centers. Therefore, it is a chiral structure. One side of the torus contains primary hydroxyl groups, whereas the secondary hydroxyl groups are located on the other side. The toroidal structure has a hydrophilic surface resulting from the 2-, 3-, and 6-position hydroxyls, making them water-soluble. The cavity is composed of the glucoside oxygens and methylene hydrogens, giving it an apolar character. As a consequence, cyclodextrins can include other apolar molecules of appropriate dimensions. To a first approximation, the magnitude of binding constants correlates with the fit of the guest in the cyclodextrin cavity.<sup>1–3</sup>

A number of studies are focused on the interactions of cyclodextrins (CDs) with surfactants having a single alkyl chain.<sup>4–12</sup> However, the stoichiometry and magnitude of equilibrium constants of surfactant complexation are still controversial.<sup>5,7</sup> For instance, the 1:1 binding constants of  $\beta$ -CD with sodium dodecyl sulfate (SDS) were reported to range over 3 orders of magnitude and to be dependent on the SDS concentration,<sup>7</sup> though reasonably close values have recently been determined by several methods.<sup>11</sup> Methods of electric conductance,<sup>4,6</sup> electromotive force,<sup>8,11</sup> surface tension,<sup>7,12</sup> <sup>19</sup>F NMR,<sup>6,9</sup> ultrasonic relaxation, sound velocity,<sup>10</sup> fluorescence,<sup>5</sup>

and calorimetry<sup>11</sup> have been applied for surfactant-CD complexation, though very few spectroscopic studies have been carried out on molecular or atomic level.<sup>6,9</sup> Such spectroscopic studies have been reported extensively for aromatic compounds.<sup>13–16</sup> No study has been done for surfactants having double alkyl chains, though it will provide new challenges in cyclodextrin chemistry.

Cyclodextrins can give beneficial modifications of guest molecules not otherwise achievable: solubility enhancement, stabilization of labile guests, control of volatility and sublimation, and physical isolation of incompatible compounds. Since they are water-soluble and practically nontoxic, they are added into pharmaceuticals and foods, for example, for stabilization of labile compounds and long-term protection of color, odor, and flavor.<sup>1–3</sup> One of the toxicities of CDs is hemolysis.<sup>3</sup> Parenteral administration of CDs is restricted by their renal (nephrotoxic) and hemolytic effects. Uekama et al. reported that cyclodextrins at lower concentrations (5 mmol dm<sup>-3</sup> for  $\alpha$ -CD and 10 mmol dm<sup>-3</sup> for  $\gamma$ -CD) protect the human erythrocytes against osmotic and heat-induced hemolysis. At higher concentrations (above 3 mmol dm<sup>-3</sup> for  $\beta$ -CD, 6 mmol dm<sup>-3</sup> for  $\alpha$ -CD, and 16 mmol dm<sup>-3</sup> for  $\gamma$ -CD), at 37 °C, pH 7.4 in 10 mmol dm<sup>-3</sup> isotonic phosphate buffer, they cause the release of cholesterol from the cell membrane in the order  $\beta$ -,  $\gamma$ -, and  $\alpha$ -CD. This indicates that the induced hemolysis is a

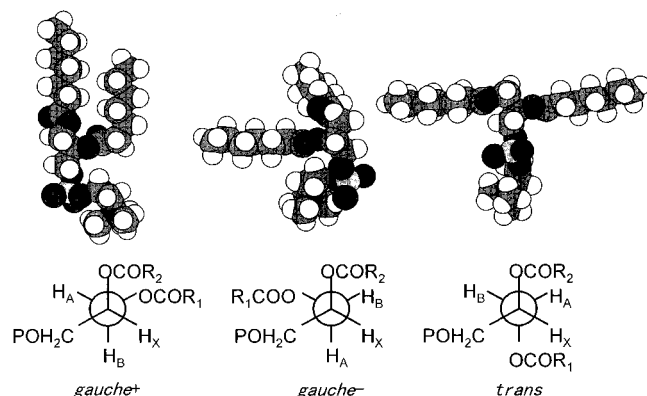


Figure 1. Definition of three rotamers of DHPC.

secondary event, resulting from the interaction of CD and membrane components. At these higher concentrations cholesterol and phospholipids are sequestered from the membrane, resulting in its disruption.<sup>17,18</sup>

In this work we investigate the complex formation of 1,2-diheptanoyl-3-L- $\alpha$ -phosphatidylcholine (DHPC) with  $\alpha$ -CD and  $\gamma$ -CD by  $^1\text{H}$  NMR. Since the length of the hexyl group is close to the depth of the CD cavity, we chose DHPC as phospholipid having double alkyl chains. This results in a reduction of the number of complex species and leads to a simple and clear analysis of observed data. The concentration of DHPC is kept constant at  $1.00 \text{ mmol kg}^{-1}$ , which is below the critical micelle concentration of about  $1.5 \text{ mmol dm}^{-3}$ ,<sup>19</sup> while the concentration of CD is increased up to  $70 \text{ mmol kg}^{-1}$ . The equilibrium binding constants (macroconstants and microconstants) of DHPC are determined, and the three-dimensional structures of their complexes are proposed on the basis of the NMR data.

### Theoretical Principle

**Three Rotamers and Vicinal Proton-Proton Coupling Constants around the C1-C2 Bond of the Glycerol Group of DHPC.** As Figure 1 shows, we can assume three rotational conformations of DHPC with different dihedral angles around the C1-C2 axis of the glycerol group: *gauche*<sup>+</sup> (*G*<sup>+</sup>), *gauche*<sup>-</sup> (*G*<sup>-</sup>), and *trans* (*T*). The proton signal of  $\text{CH}_X$  may be split into a complicated multiplet, whereas each of the proton signals of  $\text{H}_A$  and  $\text{H}_B$  may be split into a doublet due to spin-spin interactions with  $\text{H}_X$ . From the observed vicinal coupling constants of  $^3J_{AX}$  and  $^3J_{BX}$  for the spin system  $\text{CH}_A\text{H}_B - \text{CH}_X$ , we can determine the populations of these rotamers. If the rotation about the C1-C2 axis is rapid, we can regard the observed coupling constant as the average of the coupling constants for the three rotamers weighted by their populations  $P_{G^+}$ ,  $P_{G^-}$ , and  $P_T$ :

$$\begin{pmatrix} J_{AX} \\ J_{BX} \\ 1 \end{pmatrix} = \begin{pmatrix} J_{AXT} & J_{AXG^+} & J_{AXG^-} \\ J_{BXT} & J_{BXG^+} & J_{BXG^-} \\ 1 & 1 & 1 \end{pmatrix} \begin{pmatrix} P_T \\ P_{G^+} \\ P_{G^-} \end{pmatrix} = \mathbf{J} \begin{pmatrix} P_T \\ P_{G^+} \\ P_{G^-} \end{pmatrix} \quad (1)$$

Here we can employ literature coupling constant values (Hz) of  $J_{AXG^+} = 12$ ,  $J_{AXG^-} = 0.45$ ,  $J_{AXT} = 5.8$ ,  $J_{BXG^+} = 2.4$ ,  $J_{BXG^-} = 2.4$ , and  $J_{BXT} = 11.7$ .<sup>20,21</sup> Thus, the major component of  $J_{AX}$  is the *G*<sup>+</sup> form and that of  $J_{BX}$  is the *T* form.

From observed coupling constants of  $J_{AX}$  and  $J_{BX}$ , we can calculate the populations of the three rotamers:

$$\begin{pmatrix} P_T \\ P_{G^+} \\ P_{G^-} \end{pmatrix} = \mathbf{J}^{-1} \begin{pmatrix} J_{AX} \\ J_{BX} \\ 1 \end{pmatrix} \quad (2)$$

DHPC has a large number of single bonds in addition to the C1-C2 bond. We neglect the conformations formed by the internal rotation around all the bonds except for the C1-C2 bond, since these rotamers would not strikingly influence the capability of CD complexation, and they would not be major conformers.

**Equilibrium Binding Constants of DHPC for Cyclodextrins.** One or two of the heptanoyl groups of DHPC will be incorporated into the hydrophobic CD cavity. Since the length of the heptanoyl group is close to the height of the CD cavity, 1:1 and 1:2 complexes of DHPC and CD would be formed. We do not take into consideration the 2:1 complex, since we deal with the case of excess CD over DHPC. We must consider the difference between two heptanoyl groups bound to the C1 and C2 atoms of DHPC, if we can distinguish between these groups with the NMR spectrometer used. Furthermore, we do not consider theoretically which side of the primary hydroxyl groups and the secondary hydroxyl groups of CD is the binding direction of DHPC. Probably, the secondary side is preferred to the primary side, since the opening of the former is wider than the latter.

Under these conditions we define the equilibrium macroconstants of complex formation of DHPC (*L*) and CD (*D*).



$$[LD] = K_1[L][D] \quad (4)$$



$$[LD_2] = K_2[LD][D] = K_1K_2[L][D]^2 \quad (6)$$

The total concentrations of DHPC and CD are written as follows:

$$C_L = [L] + [LD] + [LD_2] = [L] + K_1[L][D] + K_1K_2[L][D]^2 \quad (7)$$

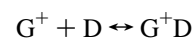
$$C_D = [D] + [LD] + 2[LD_2] = [D] + K_1[L][D] + 2K_1K_2[L][D]^2 \quad (8)$$

Removing the concentration,  $[L]$ , of free DHPC from eqs 7 and 8, we can obtain the following cubic equation with respect to the concentration,  $[D]$ , of free CD:

$$K_1K_2[D]^3 + \{K_1 + K_1K_2(2C_L - C_D)\}[D]^2 + \{1 + K_1(C_L - C_D)\}[D] - C_D = 0 \quad (9)$$

We can solve this equation for a given set of  $K_1$ ,  $K_2$ ,  $C_L$ , and  $C_D$  using the Cardano formula,<sup>22</sup> to obtain the concentrations of *D*, *L*, *LD*, and *LD*<sub>2</sub>.

Furthermore, we can calculate the concentrations of the three rotamers (*G*<sup>+</sup>, *G*<sup>-</sup>, and *T*) of DHPC in the uncomplexed form *L*, the binary complex *LD*, and the ternary complex *LD*<sub>2</sub>. The concentration of *L* can be separated into the concentrations of the three rotamers,  $[G^+]$ ,  $[G^-]$ , and  $[T]$ . Similarly, the concentrations of *LD* and *LD*<sub>2</sub> are separated into the concentrations of three rotamers, respectively. Using these concentrations, we can define six equilibrium microconstants of CD complexation with specific rotamers. For instance, the microconstant of equimolar complexation of CD and *G*<sup>+</sup> is defined as



$$K_{1G+} = [G^+D]/[G^+][D] = x_{2G+}[LD]/x_{1G+}[L][D] = x_{2G+}K_1/x_{1G+} \quad (10)$$

Similarly, other equimolar microconstants are defined as

$$K_{1G-} = [G^-D]/[G^-][D] = x_{2G-}K_1/x_{1G-} \quad (11)$$

$$K_{1T} = [TD]/[T][D] = x_{2T}K_1/x_{1T} \quad (12)$$

Here  $x$  stands for the mole fraction of each complex species, and these mole fractions are connected by the equations of  $x_{1G+} + x_{1G-} + x_{1T} = 1$  and  $x_{2G+} + x_{2G-} + x_{2T} = 1$ . We can determine the mole fractions ( $x_{1G+}$ ,  $x_{1G-}$ , and  $x_{1T}$ ) of three rotamers in uncomplexed DHPC molecules from observed coupling constants of DHPC in the absence of CD. Furthermore, we can calculate the microconstants of three ternary complexations from the equations of  $K_{2G+} = x_{3G+}K_2/x_{2G+}$ ,  $K_{2G-} = x_{3G-}K_2/x_{2G-}$ , and  $K_{2T} = x_{3T}K_2/x_{2T}$ . From these microconstants we can evaluate the affinity of each rotamer to CD. The conformational changes of DHPC induced by CD complexation are evaluated from the overall population of each rotamer:

$$P_{G+} = ([G^+] + [G^+D] + [G^+D_2])/C_L \quad (13)$$

$$P_{G-} = ([G^-] + [G^-D] + [G^-D_2])/C_L \quad (14)$$

$$P_T = ([T] + [TD] + [TD_2])/C_L \quad (15)$$

We presume that the complexation of DHPC and CD and the rotational isomerization of DHPC are both rapid on the NMR time scale. Under these conditions the chemical shift of DHPC can be written as

$$\delta_L = ([L]\delta_{L-L} + [LD]\delta_{L-LD} + [LD_2]\delta_{L-LD_2})/C_L \quad (16)$$

Here  $\delta_{L-L}$  denotes the average chemical shift of a DHPC proton for the rotational-equilibrium mixture of uncomplexed DHPC molecules, and it can be obtained from NMR spectra of DHPC in the absence of CD. Similarly,  $\delta_{L-LD}$  and  $\delta_{L-LD_2}$  denote the chemical shifts of the rotational-equilibrium mixtures of the binary and ternary complexes, respectively. For the chemical shift of a CD proton, we can write the corresponding equation:

$$\delta_D = ([D]\delta_{D-D} + [LD]\delta_{D-LD} + 2[LD_2]\delta_{D-LD_2})/C_D \quad (17)$$

To determine unknown parameters in the above equations, we compare theoretical values with observed values for the chemical shifts of DHPC and/or CD and the vicinal coupling constants of DHPC:

$$SS_1 = \sum_{n_1} (\delta_{\text{calc}} - \delta_{\text{obsd}})^2 \quad (18)$$

$$SS_2 = \sum_{n_2} (J_{\text{AXcalc}} - J_{\text{AXobsd}})^2 + \sum_{n_3} (J_{\text{BXcalc}} - J_{\text{BXobsd}})^2 \quad (19)$$

Here the theoretical values for  $\delta_L$  and  $\delta_D$  are calculated from eqs 16 and 17 and the theoretical values for  $J_{\text{AX}}$  and  $J_{\text{BX}}$  are calculable from eq 1. The fitting procedure will be explained in detail below.

If we can distinguish the chemical shifts of chains 1 and 2 of DHPC, we may determine the equilibrium microconstants of CD complexation of these chains separately. Then the binary complex defined above can be separated into two species, 1LD and 2LD, which stand for binary CD complexes with bound

chains 1 and 2, respectively. The microconstants of complexation of these chains can be defined as

$$K_{11} = [1LD]/[L][D] \quad (20)$$

$$K_{12} = [2LD]/[L][D] \quad (21)$$

Here [1LD] denotes the concentration of the binary complex 1LD possessing bound chain 1 and [2LD] has the same meaning for chain 2 with [1LD]. These microconstants are connected with the macroconstant by the equation  $K_1 = K_{11} + K_{12}$ .

The chemical shift  $\delta_{1L}$  of a chain 1 proton may be expressed as

$$\begin{aligned} C_L\delta_{1L} &= [L]\delta_{1L-L} + [1LD]\delta_{1L-LD} + [2LD]\delta_{1L-LD'} + [LD_2]\delta_{1L-LD_2} \\ &= [L]\delta_{1L-L} + K_{11}[L][D]\delta_{1L-LD} + (K_1 - K_{11})[L][D]\delta_{1L-LD'} + K_1K_2[L][D]^2\delta_{1L-LD_2} \end{aligned} \quad (22)$$

Here  $\delta_{1L-LD'}$  denotes the chemical shift of an unbound chain 1 proton of the binary complex 2LD. The other symbols in eq 22 have similar meanings. For the chemical shift of a chain 2 proton, we can write the corresponding equation:

$$\begin{aligned} C_L\delta_{2L} &= [L]\delta_{2L-L} + (K_1 - K_{11})[L][D]\delta_{2L-LD} + \\ &K_{11}[L][D]\delta_{2L-LD'} + K_1K_2[L][D]^2\delta_{2L-LD_2} \end{aligned} \quad (23)$$

Equations 22 and 23 have seven unknown independent parameters:  $K_{11}$ ,  $\delta_{1L-LD}$ ,  $\delta_{1L-LD'}$ ,  $\delta_{1L-LD_2}$ ,  $\delta_{2L-LD}$ ,  $\delta_{2L-LD'}$ , and  $\delta_{2L-LD_2}$ . Regarding them as adjustable parameters, we can calculate theoretical values of  $\delta_{1L}$  and  $\delta_{2L}$ . Thus we can fit these chemical shifts to observed values by minimizing the following  $SS_{12}$  value:

$$SS_{12} = \sum_{n_{12}} (\delta_{1L\text{calc}} - \delta_{1L\text{obsd}})^2 + \sum_{n_{12}} (\delta_{2L\text{calc}} - \delta_{2L\text{obsd}})^2 \quad (24)$$

Furthermore we can calculate the microconstants,  $K_{21}$  and  $K_{22}$ , of ternary complexation defined as follows:  $K_{21} = [LD_2]/[1LD][D]$  and  $K_{22} = [LD_2]/[2LD][D]$ . These microconstants are related with the macroconstant as  $1/K_2 = 1/K_{21} + 1/K_{22}$  and are related with the other microconstants as  $K_{11}K_{21} = K_{12}K_{22}$ .

We can consider six species of binary complexes for DHPC and CD:  $1G^+D$ ,  $1G^-D$ ,  $1TD$ ,  $2G^+D$ ,  $2G^-D$ , and  $2TD$ . In principle, we can determine the concentrations of these six species separately, if the chemical shifts for chains 1 and 2 and the vicinal coupling constants  $J_{\text{AX}}$  and  $J_{\text{BX}}$  are determined very accurately.

## Experimental Section

**NMR Measurements.** 1,2-Diheptanoyl-3-L- $\alpha$ -phosphatidylcholine (DHPC) from Sigma Chemical Co. and  $\alpha$ - and  $\gamma$ -cyclodextrins from Nacalai Tesque Co. were used as received.

All proton NMR spectra were recorded with a Varian XL-300 NMR spectrometer at 300 MHz and  $21.0 \pm 0.5$  °C. All obtained spectra were deconvoluted with a Nuts NMR data-processing software (Acorn NMR Inc.). The chemical shift of a sample in deuterium oxide was measured against sodium 3-(trimethylsilyl)propanesulfonate (TSS) as external standard. The concentration,  $C_L$ , of DHPC was kept at  $1.00 \text{ mmol kg}^{-1}$ , which is below a critical micelle concentration of  $1.5 \text{ mmol kg}^{-1}$ ,<sup>19</sup> whereas the concentration,  $C_D$ , of CD was changed up to ca.  $70 \text{ mmol kg}^{-1}$ . As some authors have already reported, the chemical shifts of all protons of CDs decreased slightly with increasing CD concentration, and the data were corrected for

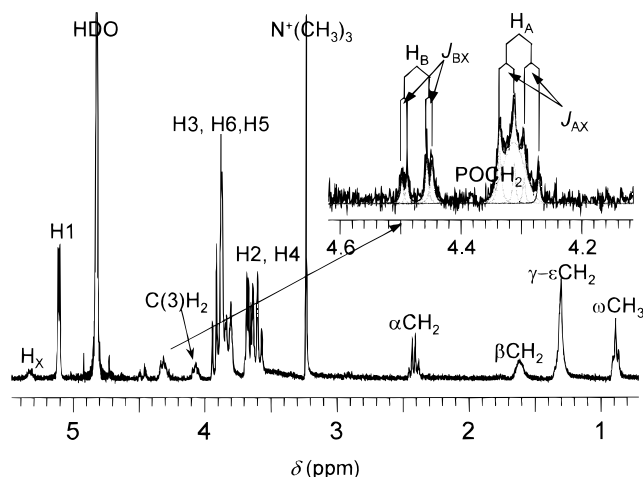


**Figure 2.** NMR spectrum of an equimolar mixture of DHPC and  $\gamma$ -CD in  $D_2O$  at  $C_L = C_D = 1 \text{ mmol kg}^{-1}$ .

this effect.<sup>16</sup> Although the reason for such a concentration dependence of CD chemical shifts is unknown, these authors ascribed it to the dimerization of CD.<sup>16</sup> Very recently, Matsui and Tokunaga have argued that the internal reference method using noncomplexing solutes is more reliable than the external one.<sup>23</sup> We actually confirmed some of their observations. Although we employed the external reference method, our chemical shift data are consistent with their internal reference ones using tetramethylammonium chloride. It was difficult to determine the coupling constants at CD concentrations higher than ca.  $20 \text{ mmol kg}^{-1}$  for  $\alpha$ -CD and  $36 \text{ mmol kg}^{-1}$  for  $\gamma$ -CD.

**Molecular Modeling of Complexes.** The literature crystal structures of  $\alpha$ -CD,<sup>24</sup>  $\gamma$ -CD,<sup>25</sup> and DHPC<sup>19,26,27</sup> were regarded as rigid bodies unchanged with their complexation; the structure of DHPC was actually inferred from the crystal structure of dimyristoylphosphatidylcholine. The rotamer of DHPC in the crystal will be the  $G^+$  form, in which the 2-heptanoyl chain has a cis segment (Figure 1). The 2-heptanoyl chain in the  $G^-$  and T forms was regarded as a fully extended conformation (Figure 1), although it may be somewhat folded in the uncomplexed form, because of intramolecular hydrophobic interactions between the two heptanoyl chains.<sup>21</sup> A HyperChem (Hypercube, Inc., Canada) package modeling software and our own modeling software<sup>19</sup> were used to model the complexes of DHPC and CDs. The structures of the complexes were not energy-minimized. Molecular modeling and data analysis were carried out with an NEC PC-9821 Ra20/N12 computer (Pentium Pro processor/200 MHz) and a Compaq Deskpro XL 5100 computer using Microsoft Excel Version 7.0 for Windows 95.

## Results

**Chemical Shifts of DHPC and CD.** Figure 2 displays the 300-MHz  $^1H$  NMR spectrum of a deuterium oxide solution containing  $1 \text{ mmol kg}^{-1}$  DHPC and  $1 \text{ mmol kg}^{-1}$   $\gamma$ -CD. The assignment of each proton of DHPC and the CD was carried out in comparison with the literature spectra of short-chain lecithins<sup>20,21</sup> and  $\alpha$ -CD.<sup>13</sup>

The H1 protons of  $\gamma$ -CD appeared near 5.1 ppm, the protons of H3, H5, and H6 resonated around 3.85 ppm, and those of H2 and H4 were assigned to the peaks centered at 3.6 ppm. The H1, H2, and H4 protons are located on the outer surface of the CD cavity, whereas those of H3 and H5 are on the inner surface of CD. The spectrum of  $\alpha$ -CD was akin to that of  $\gamma$ -CD.

The  $H_X$  proton of the  $C2H_X$  fragment of DHPC exhibits a complicated multiplet at 5.3 ppm. The  $H_B$  and  $H_A$  protons of

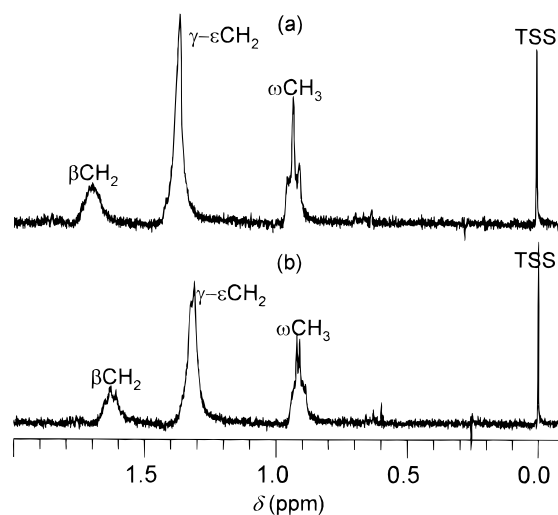
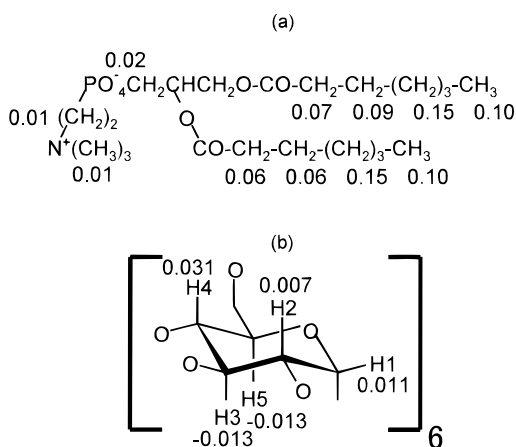


**Figure 3.** Nonequivalence of methyl and intermediate methylene protons of DHPC induced by the addition of  $\gamma$ -CD: spectra of (a) a  $1 \text{ mmol kg}^{-1}$  DHPC solution and (b) a  $1 \text{ mmol kg}^{-1}$  DHPC solution containing  $7 \text{ mmol kg}^{-1}$   $\gamma$ -CD.

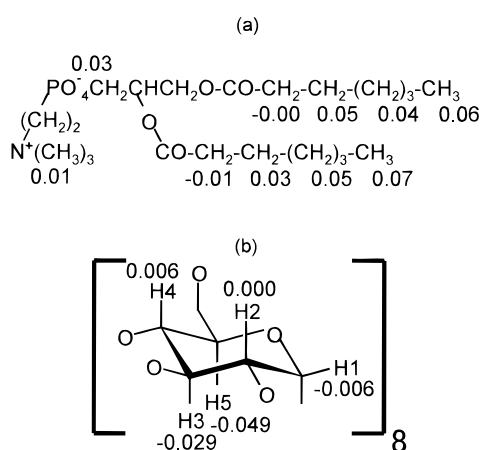
the  $C1H_AH_B$  fragment, though their spectrum is also shown in an expanded scale, appeared as quartets at 4.5 and 4.3 ppm, respectively. The  $H_A$  proton was overlapped with part of the protons of  $C3OPOCH_2$ . The peaks at 4.1 ppm were assigned to the protons of  $C3H_2OP$ . The trimethyl protons of the choline group exhibit a sharp singlet at 3.2 ppm. The protons of two hexyl groups exhibited four main peaks at high fields. The protons of two  $\alpha$ - $CH_2$  groups were split into double triplets apparently like a quartet. The triplet at a higher field was assigned to the  $\alpha$ -methylene protons of chain 1, whereas the triplet at a lower field was assigned to those of chain 2.<sup>21,28</sup> Hereafter, we assume that the protons of chain 1 appeared at a higher field than those of chain 2. Although the protons of two  $\beta$ - $CH_2$  groups were apparently a multiplet, those peaks are actually composed of double multiplets. The protons of the intermediate methylene groups ( $\gamma$ -,  $\delta$ -, and  $\epsilon$ - $CH_2$  groups) appeared to be a broad tall peak. The protons of the  $\omega$ -methyl groups of DHPC exhibited a single triplet at the highest field in our mixture system. All of the above peaks did not overlap with those of CD. The peaks of the methylene protons adjacent to the choline group positioned around 3.7 ppm were buried in peaks of CD.

Figure 3 shows the spectral changes of the terminal methyl and intermediate methylene protons of DHPC with the addition of  $\gamma$ -CD. The proton peaks of these groups were split into more peaks owing to the magnetic nonequivalence of chains 1 and 2 induced by  $\gamma$ -CD. This induced nonequivalence reflects the difference between the environments of chains 1 and 2 bound to  $\gamma$ -CD. A similar splitting of the protons of the two terminal methyl groups of dihexanoyllecithin was observed, when it formed micelles.<sup>28</sup>

Figures 4 and 5 show the variation in chemical shift of the peaks of DHPC and CD with the addition of  $\alpha$ - or  $\gamma$ -CD to a  $1 \text{ mmol kg}^{-1}$  DHPC solution. The negative variation indicates a decrease in chemical shift  $\delta$ , viz., a shift toward a high field, and vice versa. As a first approximation, the magnitude of these variations in chemical shift reflects the proximity of DHPC and CD. In Figures 4 and 5, the chemical shift variations of the protons of the hexyl groups of DHPC are much larger than those of the glycerophosphocholine group, indicating that the hydrophobic former groups are included into the CD cavity. The chemical shift variations for  $\alpha$ -CD exceed those for  $\gamma$ -CD. The main reason for this difference will be that  $\alpha$ -CD contacts with



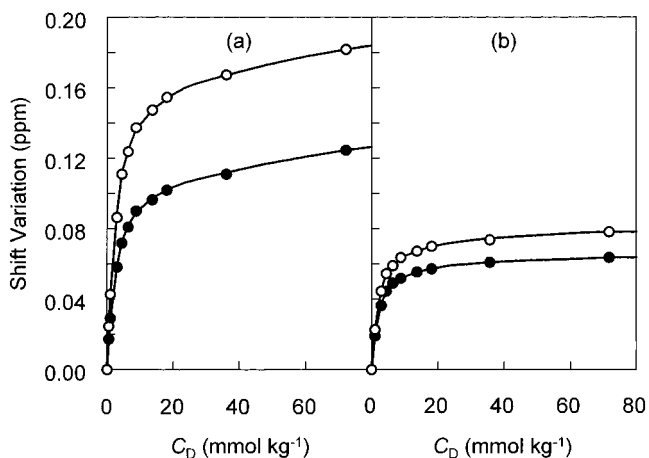
**Figure 4.** Changes in chemical shift of each proton of (a) DHPC on the addition of 18 mmol kg<sup>-1</sup> α-CD to a 1 mmol kg<sup>-1</sup> DHPC solution and (b) α-CD on decreasing the α-CD concentration from 72 to 1 mmol kg<sup>-1</sup> in a 1 mmol kg<sup>-1</sup> DHPC solution.



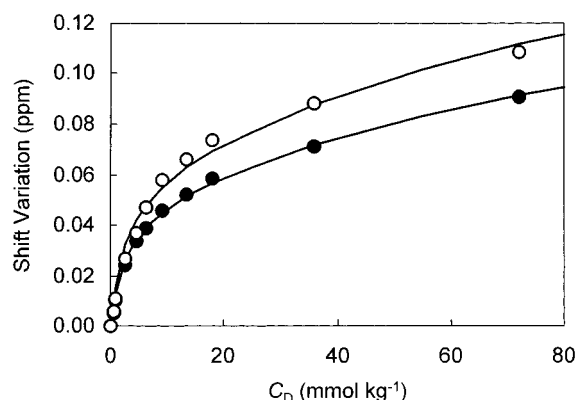
**Figure 5.** Changes in chemical shift of each proton of (a) DHPC on the addition of 18 mmol kg<sup>-1</sup> γ-CD into a 1 mmol kg<sup>-1</sup> DHPC solution and (b) γ-CD on decreasing the γ-CD concentration from 72 to 1 mmol kg<sup>-1</sup> in a 1 mmol kg<sup>-1</sup> DHPC solution.

the hexyl group more closely than γ-CD, since the former cavity is smaller than the latter. Regardless of chains 1 and 2 for α-CD, the variations for the intermediate methylene groups are greatest among those for the hexyl group, suggesting that these groups are located in the center of the α-CD cavity. On the other hand, for γ-CD, the terminal methyl groups exhibit the greatest variations, suggesting that these groups center in the γ-CD cavity. The α-methylene groups are not incorporated in the γ-CD cavity, since the variations of these groups are negligible. As Figure 5 shows, the variations in chemical shift of the intermediate methylene protons and the terminal methyl protons are different with chains 1 and 2. In the solutions containing 18 mmol kg<sup>-1</sup> α- or γ-CD and 1 mmol kg<sup>-1</sup> DHPC, 90% or more of the DHPC molecules complex with CD, as will be shown later.

For both α-CD and γ-CD, the inner protons H3 and H5 shifted toward higher fields, whereas the outer protons H2 and H4 shifted toward lower fields. The absolute variations for the inner protons of γ-CD are greater than those for the inner protons of α-CD, suggesting that both of the two hexyl groups of DHPC are accommodated in one γ-CD cavity. Regarding the outer protons, α-CD exhibits larger shifts than γ-CD. As a result of a deeper penetration of DHPC into the α-CD cavity, the outer protons may contact more closely with the glycerophosphocholine group or the free hexyl chain.



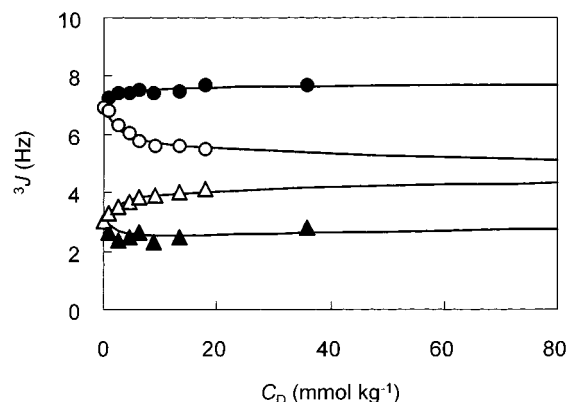
**Figure 6.** Concentration dependence of chemical shift variations of (a) the intermediate methylene protons (○) and methyl protons (●) of DHPC in α-CD solutions and (b) the terminal methyl protons in chain 2 (○) and chain 1 (●) in γ-CD solutions. The solid lines were calculated from eq 16 and 17 on the basis of the binding model using the parameters shown in Table 1.



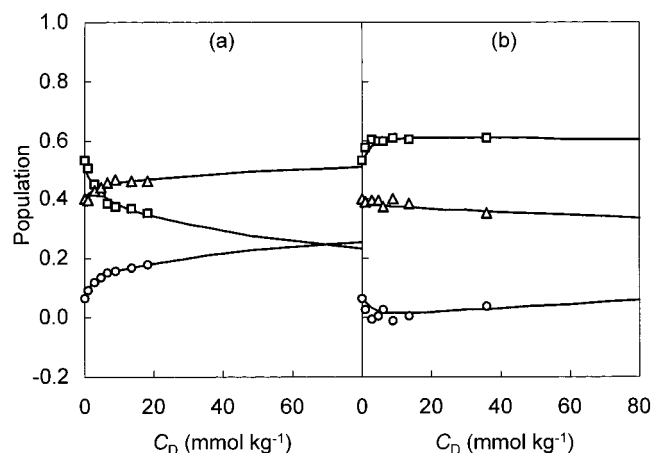
**Figure 7.** Concentration dependence of chemical shift variations for α-methylene protons of chain 1 (○) and chain 2 (●) of DHPC. The solid lines were calculated from eq 24 using the parameters shown in Tables 1 and 2.

Figure 6 illustrates the CD concentration dependence of chemical shifts of (a) the intermediate methylene protons and terminal methyl protons in α-CD solutions and (b) those of the terminal methyl protons of chains 1 and 2 in γ-CD solutions. These protons vary largely with the addition of α-CD and γ-CD and do not overlap with other protons. Figure 7 shows the dependence of chemical shift variations of the α-methylene protons of chains 1 and 2 on the α-CD concentration. The assignment of these protons of DHPC has been established separately for chains 1 and 2.<sup>21,28</sup>

**Vicinal Coupling Constants of the C1H<sub>2</sub>-C2H Bond of DHPC.** As Figure 2 shows, the peak of proton H<sub>A</sub>, though overlapped with the peaks of the C3OPOCH<sub>2</sub> protons, is split into a quartet. This splitting is due to the coupling with the geminal proton H<sub>B</sub> and the vicinal proton H<sub>X</sub>. We used the average of two values of the vicinal coupling constant  $J_{AX}$  for further analysis. Similarly, we used the average  $J_{BX}$  value obtained from the quartet of proton H<sub>B</sub>, resulting from the coupling with the geminal proton H<sub>A</sub> and the vicinal proton H<sub>X</sub>. Our coupling constants for DHPC,  $J_{AB} = 12.2$  Hz,  $J_{AX} = 6.8$  Hz, and  $J_{BX} = 3.1$  Hz, are very close to literature values of  $J_{AB} = 12.0$  Hz,  $J_{AX} = 6.8$  Hz, and  $J_{BX} = 3.0$  Hz for dihexanoylphosphatidylcholine in D<sub>2</sub>O.<sup>21</sup> The populations of three rotamers of DHPC, calculated from our coupling constants, are  $P_{G+} = 0.515$ ,  $P_{G-} = 0.406$ , and  $P_T = 0.079$ .



**Figure 8.** Concentration dependence of vicinal coupling constants of the  $\text{CH}_A\text{H}_B\text{CH}_X$  system of DHPC:  $J_{AX}$  in  $\alpha$ -CD solutions (○) and in  $\gamma$ -CD solutions (●) and  $J_{BX}$  in  $\alpha$ -CD solutions (Δ) and in  $\gamma$ -CD solutions (▲). The solid lines were calculated from eq 1 using the parameters shown in Table 1.



**Figure 9.** Populations of the rotational isomers  $G^+$  (□),  $G^-$  (Δ), and T (○), calculated from eq 2 using the observed coupling constant data (Figure 8), as a function of the concentration of (a)  $\alpha$ -CD and (b)  $\gamma$ -CD. The solid lines were calculated from the equilibrium microconstants and the mole fractions shown in Table 1.

As Figure 8 shows, the concentration dependence of the coupling constants,  $J_{AX}$  and  $J_{BX}$ , for  $\alpha$ -CD is almost opposite to that for  $\gamma$ -CD. This fact shows that the three rotamers of DHPC (Figure 1) have quite different affinities to  $\alpha$ -CD and  $\gamma$ -CD. The decrease in  $J_{AX}$  and the increase in  $J_{BX}$  for  $\alpha$ -CD solutions indicate an increase of the T form and a decrease of the  $G^+$  form. On the other hand, the increase in  $J_{AX}$  and the initial decrease and final increase in  $J_{BX}$  for  $\gamma$ -CD solutions indicate an increase of the  $G^+$  form and an initial decrease and a final increase of the T form. It was difficult to determine the coupling constants at very high concentrations. Figure 9 shows the populations of three rotamers, calculated from eq 2, as a function of the CD concentration. These results show how the conformation of DHPC changes with CD complexation and which conformer of DHPC binds preferentially with CD. Here it should be noted that the population of the  $G^-$  form is the most unreliable among all populations: the populations of the T and  $G^+$  forms are directly calculable from the observed vicinal coupling constants, but that of the  $G^-$  form is the rest.

**Estimation of Binding Constants and Population of Each Complex Species.** We estimated the macroconstants and microconstants of complexation by the following three steps. First, we estimated the equilibrium macroconstants  $K_1$  and  $K_2$  using the chemical shift data shown in Figure 6. Then we estimated the mole fractions of three rotamers of DHPC using

**TABLE 1: Equilibrium Macro- and Microconstants, Mole Fractions, and Variations of Chemical Shifts of DHPC Protons for  $\alpha$ -CD and  $\gamma$ -CD**

parameters	$\alpha$ -cyclodextrin	$\gamma$ -cyclodextrin
$n_1$	20 <sup>a</sup>	18 <sup>a</sup>
$n_2$	7 <sup>b</sup>	8 <sup>b</sup>
$n_3$	7 <sup>b</sup>	7 <sup>b</sup>
$K_1$ (kg mol <sup>-1</sup> )	550	748
$K_2$ (kg mol <sup>-1</sup> )	8.62	1.92
$\Delta\delta_{LD}(\text{CH}_2)_{\gamma-\epsilon}$	0.161	
$\Delta\delta_{LD2}(\text{CH}_2)_{\gamma-\epsilon}$	0.214	
$\Delta\delta_{LD}(\text{CH}_3)$	0.105	
$\Delta\delta_{LD2}(\text{CH}_3)$	0.157	
$\Delta\delta_{LD}(1\text{-CH}_3)$		0.060
$\Delta\delta_{LD}(2\text{-CH}_3)$		0.074
$\Delta\delta_{LD2}(1\text{-CH}_3)$		0.095
$\Delta\delta_{LD2}(2\text{-CH}_3)$		0.122
$x_{1G+}$	0.515	0.515
$x_{1G-}$	0.406	0.406
$x_{1T}$	0.079	0.079
$x_{2G+}$	0.384	0.623
$x_{2G-}$	0.457	0.377
$x_{2T}$	0.159	0.000
$x_{3G+}$	0.000	0.479
$x_{3G-}$	0.591	0.069
$x_{3T}$	0.409	0.453
$K_{1G+}$ (kg mol <sup>-1</sup> )	410	905
$K_{1G-}$ (kg mol <sup>-1</sup> )	620	696
$K_{1T}$ (kg mol <sup>-1</sup> )	1100	$1.02 \times 10^{-5}$
$K_{2G+}$ (kg mol <sup>-1</sup> )	0.00	1.48
$K_{2G-}$ (kg mol <sup>-1</sup> )	11.1	0.35
$K_{2T}$ (kg mol <sup>-1</sup> )	22.2	$8.12 \times 10^8$

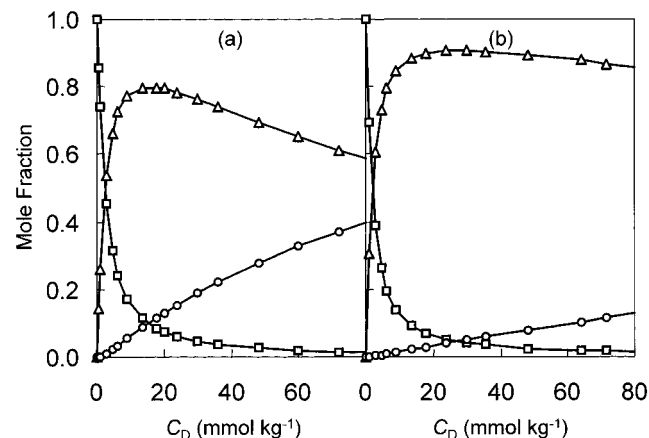
<sup>a</sup> Number of data defined in eq 18. <sup>b</sup> Number of data defined in eq 19.

the vicinal coupling constant data shown in Figure 8. Finally, the affinities of chains 1 and 2 of DHPC to  $\alpha$ -CD were estimated using the chemical shift data shown in Figure 7.

For  $\alpha$ -CD we have 10 pairs of the observed chemical shifts of the intermediate methylene protons and the terminal methyl protons, shown in Figure 6a. To calculate the corresponding chemical shifts, we regarded  $K_1$  and  $K_2$  of eq 9 and  $\delta_{L-LD}$  (or  $\Delta\delta_{L-LD} = \delta_{L-LD} - \delta_{L-L}$ ) and  $\delta_{L-LD2}$  (or  $\Delta\delta_{L-LD2} = \delta_{L-LD2} - \delta_{L-L}$ ) of eq 16 for two pairs of protons as six adjustable parameters. Thus, we obtained the best fit values of these six parameters for  $\alpha$ -CD shown in Table 1. Next, to calculate six microconstants  $K_{1G+}$ ,  $K_{1G-}$ ,  $K_{1T}$ ,  $K_{2G+}$ ,  $K_{2G-}$ , and  $K_{2T}$ , we used the observed populations of three rotamers for the free DHPC molecule ( $x_{1G-}$ ,  $x_{1G+}$ , and  $x_{1T}$ ), the estimated macroconstants ( $K_1$  and  $K_2$ ), and seven pairs of observed vicinal coupling constants,  $J_{AX}$  and  $J_{BX}$ . To calculate 14 values of the corresponding coupling constants, we regarded  $x_{2G+}$ ,  $x_{2G-}$ ,  $x_{3G+}$ , and  $x_{3G-}$  in eq 2 and 13–15 as four adjustable parameters, although these mole fractions are not explicitly written in these equations. These estimated mole fractions and microconstants are shown in Table 1. Furthermore, we tried to determine the equilibrium microconstants for chains 1 and 2 of DHPC separately. The 20 observed chemical shift variations for two pairs of the  $\alpha$ -methylene protons shown in Figure 7 were used to obtain information on the preference of chains 1 and 2 to bind to  $\alpha$ -CD, although these values are less accurate than those of the intermediate methylene and terminal methyl protons. The corresponding theoretical values were calculated from eq 22 using the estimated macroconstants ( $K_1$  and  $K_2$ ) and a reasonable assumption of  $\delta_{LD2} = \delta_{LD}$  for both chains 1 and 2. The best fit values of two microconstants  $K_{11}$  and  $K_{21}$  and four chemical shift variations for the binary and ternary complexes are shown in Table 2. There is almost no distinction between chains 1 and 2 of DHPC for binding with  $\alpha$ -CD.

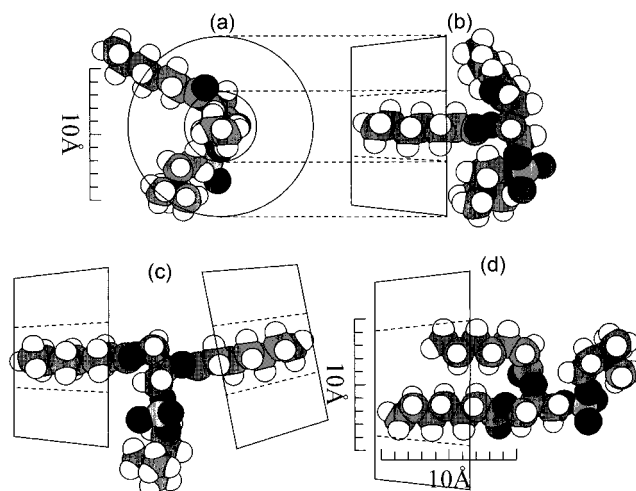
**TABLE 2: Equilibrium Microconstants and Variations of Chemical Shifts of DHPC  $\alpha$ -Methylene Protons with the Addition of  $\alpha$ -CD**

$n_{12}$	10 <sup>a</sup>	$\Delta\delta_{LD}(1-CH_2)$	0.414
$K_{11}$ (kg mol <sup>-1</sup> )	281	$\Delta\delta_{LD'}(1-CH_2)$	-0.203
$K_{12}$ (kg mol <sup>-1</sup> )	269	$\Delta\delta_{LD}(2-CH_2)$	0.340
$K_{21}$ (kg mol <sup>-1</sup> )	16.9	$\Delta\delta_{LD'}(2-CH_2)$	-0.146
$K_{22}$ (kg mol <sup>-1</sup> )	17.6		

<sup>a</sup> Number of data defined in eq 24.**Figure 10.** Concentration dependence of populations of the uncomplexed DHPC molecule ( $\square$ ), the equimolar complex ( $\Delta$ ), and the ternary complex ( $\circ$ ) for (a)  $\alpha$ -CD and (b)  $\gamma$ -CD. This dependence was calculated from the equilibrium macroconstants  $K_1$  and  $K_2$  shown in Table 1.

For  $\gamma$ -CD, we used 18 observed chemical shift data of two pairs of the terminal methyl protons (Figure 6b) to estimate the macroconstants ( $K_1$  and  $K_2$ ) of eq 9, regarding these constants and the chemical shift variations  $\Delta\delta_{L-LD}$  ( $=\delta_{L-LD} - \delta_{L-L}$ ) and  $\Delta\delta_{L-LD2}$  ( $=\delta_{L-LD2} - \delta_{L-L}$ ) for chains 1 and 2 of eq 16 as six adjustable parameters. Then we estimated the 4 independent mole fractions of three rotamers for binary and ternary complexes using 15 observed coupling constants (8  $J_{AX}$  and 7  $J_{BX}$  values). Furthermore, using these best fit values of  $K_1$ ,  $K_2$ ,  $x_{2G+}$ ,  $x_{2G-}$ ,  $x_{3G+}$ , and  $x_{3G-}$ , we calculated the microconstants  $K_{1G+}$ ,  $K_{1G-}$ ,  $K_{1T}$ ,  $K_{2G+}$ ,  $K_{2G-}$ , and  $K_{2T}$ . These values are shown in Table 1. Since the variations,  $\Delta\delta_{LD2}(1-CH_3)$  and  $\Delta\delta_{LD2}(2-CH_3)$ , of chemical shifts of the terminal methyl protons of chains 1 and 2 significantly depended on data treatments, the equilibrium microconstants for ternary complexation are not very accurate. We could not determine the equilibrium microconstants for binary complexation of chains 1 and 2 separately, since the major complex is the  $G^+$  form.

Figure 10 shows the mole fraction of each complex species as a function of CD concentration. Those mole fractions were calculated from the equilibrium macroconstants  $K_1$  and  $K_2$  (Table 1). We should keep in mind that the absolute values of the best-fit parameters shown in Tables 1 and 2 are not very reliable, although a relative comparison among these values is significant. Even the macroconstant  $K_2$  for ternary complexation is less accurate than  $K_1$  and consequently the microconstants  $K_{2G+}$ ,  $K_{2G-}$ , and  $K_{2T}$  and the mole fractions  $x_{3G+}$ ,  $x_{3G-}$ , and  $x_{3T}$  for three rotamers are much more inaccurate. The reason for this lower accuracy is that the concentrations of ternary complexes are much lower than those of binary complexes. Table 1 shows that the T conformer of DHPC more easily forms the binary and ternary complexes with  $\alpha$ -CD than the other rotamers. In Table 2 it is noted that the microconstants for binary complexation are close to each other and similar to those of surface-active substances having a single hexyl group.<sup>29-31</sup>

**Figure 11.** Proposed three-dimensional structures of three major complexes: (a) side view of  $2G^-\alpha$ -CD, (b) top view of  $2G^-\alpha$ -CD, (c)  $T(\alpha\text{-CD})_2$ , and (d)  $G^+\gamma$ -CD.

This result suggests that the two hexyl chains of DHPC can bind with  $\alpha$ -CD rather independently. For single alkyl chain surfactants, the equilibrium constant of binary complexation with  $\gamma$ -CD are smaller than that with  $\alpha$ -CD, and the equilibrium constant of their ternary complexation with  $\gamma$ -CD is larger than that of their binary complexation with  $\gamma$ -CD.<sup>7,32</sup> In Table 1, it is remarkable that the converse results were found for the complexation of DHPC and  $\gamma$ -CD.

**Molecular Structures of Complexes.** On the basis of the above results, we propose the molecular structures of two major  $\alpha$ -CD complexes and a major  $\gamma$ -CD complex in Figure 11. In the equimolar complex of DHPC with  $\alpha$ -CD, chain 2 of DHPC is presumed to be bound to  $\alpha$ -CD, although  $K_{11}$  is actually close to  $K_{12}$ . This hexyl chain is incorporated in the cavity rather deeply, since the intermediate methylene protons exhibit the greatest variation in all protons of DHPC (Figure 4). The T conformer of DHPC has the greatest affinity to  $\alpha$ -CD, as is evident from the magnitude of binary and ternary microconstants in Table 1. The H4 protons of  $\alpha$ -CD are outside of the cavity and near the secondary-hydroxyls side. The chemical shift of these protons in all CD protons varies most remarkably with complexation. This variation would be caused by the proximity of the phosphate group or the 1-hexyl group of DHPC. Since the chemical shifts of the choline trimethyl protons little varied, these protons are unlikely to be located near the H4 protons. The most preferable ternary complex of DHPC with  $\alpha$ -CD is  $T(\alpha\text{-CD})_2$  shown in Figure 11c. The relative position between the hexyl group and  $\alpha$ -CD in the binary complex  $T\alpha$ -CD will be similar to that of the binary complex  $2G^-\alpha$ -CD. The second ligation of  $\alpha$ -CD will be sterically easy to the T conformer of DHPC.

The predominant binary complex of DHPC with  $\gamma$ -CD is  $G^+\gamma$ -CD. This structure is consistent with the variation of chemical shift shown in Figure 5 and the magnitude of the binding constants shown in Table 1. The terminal methyl groups are deeply incorporated in the cavity, since the chemical shifts of these protons varied more than those of the other protons. The terminal methyl group of chain 2 is incorporated nearer the center of the cavity than that of chain 1, so that the former protons show larger chemical shift variation than the latter protons. Little varied the chemical shifts of the  $\alpha$ -methylene protons (Figure 5). The cavity of  $\gamma$ -CD is large enough to incorporate two alkyl chains simultaneously. Hence the equilibrium constant of binary complexation of DHPC with

$\gamma$ -CD exceeds that of DHPC with  $\alpha$ -CD. This is a remarkable result, since surfactants having single chains bind more strongly with  $\alpha$ -CD than with  $\gamma$ -CD.<sup>7,32</sup> Since two hexyl groups of a DHPC molecule are tightly bound to a  $\gamma$ -CD cavity, the mobility of these groups therein will be decreased, so that the protons of these groups are discriminated in their NMR spectra. The terminal methyl group of chain 1 may fold toward the center of the CD cavity.

## Discussion

The  $K_1$  value for sodium 1-hexanesulfonate<sup>4</sup> with  $\alpha$ -CD at 298 K was reported to be 379 dm<sup>3</sup> mol<sup>-1</sup> and that of 1-hexanol with  $\alpha$ -CD was 891,<sup>29</sup> 591 dm<sup>3</sup> mol<sup>-1</sup>,<sup>30</sup> and 379 kg mol<sup>-1</sup>.<sup>31</sup> These values demonstrate that the  $K_1$  value depends primarily on the alkyl chain length and secondly on the headgroup. Our values of  $K_{11}$  and  $K_{12}$  for  $\alpha$ -CD are similar to these values. For single-chain surfactants,  $\alpha$ -CD has much higher affinity than  $\gamma$ -CD and the  $K_2$  value for  $\gamma$ -CD is greater than the  $K_1$  value for  $\gamma$ -CD by one order.<sup>7,32</sup> These results are explained on the basis of the diameter of the alkyl chain and the size of the CD cavity. The alkyl chain best fits to the  $\alpha$ -CD cavity, but it is too thin to be effectively incorporated into the  $\gamma$ -CD cavity. Since two alkyl chains are fixed in the  $\gamma$ -CD cavity without room, the  $K_1$  value for DHPC with  $\gamma$ -CD is larger than that for DHPC with  $\alpha$ -CD, and single-chain surfactants are cooperatively bound to  $\gamma$ -CD ( $K_2 > K_1$ ). Some of the methods mentioned in the Introduction section may be employed to determine the macroconstants for the present systems. For instance, the surface tension method that determines the free surfactant concentration would be applicable.<sup>7,12,33</sup> This method, however, needs much larger amounts of DHPC and deuterium oxide than NMR, and these compounds are rather expensive.

The chemical shift variation of a DHPC proton with the addition of CD would be caused by at least two factors, viz., changes in environment of the probe proton and in populations of three rotamers with CD binding. The three rotamers will have different chemical shifts, and then the average of these shifts weighted by the population of each rotamer is observed. The chemical shift variation of the intermediate methylene protons in the equimolar complex is 0.161 ppm for  $\alpha$ -CD (Table 1). This value is close to a variation of 0.17 ppm for the probe proton of alkanols with the addition of  $\alpha$ -CD. The resonance of H3 of  $\alpha$ -CD shifts to higher field by  $-0.055$  ppm with the addition of DHPC (estimated from best fitting). This variation is close to a variation of  $-0.06$  ppm observed for the same protons with the addition of alkanols.<sup>31</sup> A general tendency for the sign of chemical shift variation is seen in Table 1 and Figures 4 and 5. An exception for this tendency is the negative variations of the unbound  $\alpha$ -methylene protons (Table 2). The chemical shift of these protons tends to be affected by conformational changes of DHPC, though the reason for this is unclear.

The magnetic nonequivalence of the terminal methyl and intermediate methylene groups in chains 1 and 2 induced by CD complexation may be due to a decrease in mobility and the difference in environment of these groups in the CD cavity. These groups in the unbound state will rotate rather freely, so that the protons may be located in a similar magnetic environment, regardless of chains 1 and 2. As Figure 11d shows, however, the terminal methyl group in chain 2 is closer to the center of the  $\gamma$ -CD cavity than that in chain 1. The chemical shift variation for the former, therefore, is larger than that for the latter (Figure 5).

The addition of  $\alpha$ -CD causes an increase of the T conformer of DHPC and a decrease of the G<sup>+</sup> conformer, whereas the

addition of  $\gamma$ -CD results in the converse changes. The T form rather preferentially binds to  $\alpha$ -CD to form their binary and ternary complexes. The G<sup>+</sup> form strongly binds to  $\gamma$ -CD to form their binary complex. Since the macroconstant for ternary complexation is small for both  $\alpha$ -CD and  $\gamma$ -CD, we could not determine very reliable microconstants for this reaction and the mole fractions of three rotamers in ternary complexes. In particular, the mole fraction of the G<sup>-</sup> form is less accurate than those of the T and G<sup>+</sup> forms, since the former fraction was estimated as the rest of the latter ones. Further, the mole fraction  $x_{2T}$  of T $\gamma$ -CD is almost zero (Table 1). This must lead to a too large  $K_{2T}$  value for  $\gamma$ -CD in Table 1.

Three-dimensional structures of some major complexes are proposed in Figure 11. These structures are consistent with the present results. In the binary complex G<sup>+</sup> $\alpha$ -CD, the terminal part of chain 1 in the G<sup>+</sup> form may be incorporated in the  $\alpha$ -CD cavity. In the binary complexes G<sup>+</sup> $\alpha$ -CD, G<sup>-</sup> $\alpha$ -CD, T $\alpha$ -CD, G<sup>-</sup> $\gamma$ -CD, and T $\gamma$ -CD, either chain 1 or chain 2 is bound with CD. It is therefore noted that the formation microconstants of these binary complexes,  $K_{1G^+}$  ( $\alpha$ -CD),  $K_{1G^-}$  ( $\alpha$ -CD),  $K_{1T}$  ( $\alpha$ -CD),  $K_{1G^-}$  ( $\gamma$ -CD), and  $K_{1T}$  ( $\gamma$ -CD), are about two times those when two chains are distinguished.

Mixtures of dilauroylphosphatidylcholine (DLPC) and distearoylphosphatidylcholine (DSPC) with  $\alpha$ - and  $\gamma$ -CD formed precipitates in aqueous solutions. The D:L ratios in the  $\alpha$ -CD precipitates were 4.2 and 5.5 for DLPC and DSPC, whereas those in the  $\gamma$ -CD precipitates were 1.5 and 1.8 for DLPC and DSPC.<sup>18</sup> This is explicable on the basis of the present results as follows. The main complexes of DLPC and DSPC in the  $\alpha$ -CD precipitates will be T( $\alpha$ -CD)<sub>4</sub> and T( $\alpha$ -CD)<sub>6</sub>, respectively. On the other hand, those of these lecithins in the  $\gamma$ -CD precipitates are expected to be G<sup>+</sup> $\gamma$ -CD and G<sup>+</sup>( $\gamma$ -CD)<sub>2</sub>, respectively. Here it should be noted that DLPC and DSPC have longer acyl chains than DHPC by factors of 2 and 3, respectively. This is an important prediction for understanding the mechanism of hemolysis by CDs, since the membrane of erythrocytes is composed of long-chain phospholipids.

## References and Notes

- (1) Bender, M. L.; Komiyama, M. *Cyclodextrin Chemistry*; Springer-Verlag: Berlin, 1978; Chapters 2 and 3.
- (2) Saenger, W. *Angew. Chem., Int. Ed. Engl.* **1980**, *19*, 344.
- (3) Szejtli, J. *Cyclodextrin Technology*; Kluwer Academic Publishers: Dordrecht, 1988; Chapters 2 and 3.
- (4) Satake, I.; Ikenoue, T.; Takeshita, T.; Hayakawa, K.; Maeda, T. *Bull. Chem. Soc. Jpn.* **1985**, *58*, 2746.
- (5) Park, J. W.; Song, H. J. *J. Phys. Chem.* **1989**, *93*, 6454.
- (6) Palepu, R.; Reinsborough, V. C. *Can. J. Chem.* **1989**, *67*, 1550.
- (7) Funasaki, N.; Yodo, H.; Hada, S.; Neya, S. *Bull. Chem. Soc. Jpn.* **1992**, *65*, 1323 and references therein.
- (8) Wan Yunus, W. M. Z.; Taylor, J.; Bloor, D. M.; Hall, D. G.; Wyn-Jones, E. *J. Phys. Chem.* **1992**, *96*, 8979.
- (9) Guo, W.; Fung, B. M.; Christian, S. D. *Langmuir* **1992**, *8*, 446.
- (10) Jobe, D. J.; Verrall, R. E.; Junquera, E.; Aicart, E. *J. Phys. Chem.* **1994**, *98*, 10814.
- (11) Mwakibete, H.; Cristantino, R.; Bloor, D. M.; Wyn-Jones, E.; Holzwarth, J. F. *Langmuir* **1995**, *11*, 57 and references therein.
- (12) Tuncay, M.; Christian, S. D. *J. Colloid Interface Sci.* **1994**, *167*, 181.
- (13) Wood, D. J.; Hruska, F. E.; Saenger, W. *J. Am. Chem. Soc.* **1977**, *99*, 1735.
- (14) Behr, J. P.; Lehn, J. M. *J. Am. Chem. Soc.* **1976**, *98*, 1743.
- (15) Lipkowitz, K. B.; Raghothama, S.; Yang, J. *J. Am. Chem. Soc.* **1992**, *114*, 1554.
- (16) Alston, D. R.; Lilly, T. H.; Stoddart, J. F. *J. Chem. Soc., Chem. Commun.* **1985**, 1600.
- (17) Uekama, K.; Irie, T.; Sunada, M.; Otogiri, M.; Iwasaki, K.; Okano, Y.; Miyata, T.; Kase, Y. *J. Pharm. Pharmacol.* **1981**, *33*, 707.
- (18) Miyajima, K.; Sawada, M.; Nakagaki, M. *Chem. Pharm. Bull.* **1985**, *33*, 2587.



- (19) Ishikawa, S.; Hada, S.; Funasaki, N. *J. Phys. Chem.* **1995**, *99*, 11508.
- (20) Birdsall, N. J. M.; Feeney, J.; Lee, A. G.; Metcalfe, J. C. *J. Chem. Soc., Perkin Trans 2* **1972**, 1441.
- (21) Hauser, H.; Guyer, W.; Pascher, I.; Skrabal, P.; Sundell, S. *Biochemistry* **1980**, *19*, 366.
- (22) Yano, K. *The Encyclopedia of Mathematics*; Koudansha: Tokyo, 1980; p 347.
- (23) Matsui, Y.; Tokunaga, S. *Bull. Chem. Soc. Jpn.* **1996**, *69*, 2477.
- (24) Philip, C. M.; Saenger, W. *J. Am. Chem. Soc.* **1974**, *96*, 3630.
- (25) Harata, K. *Bull. Chem. Soc. Jpn.* **1987**, *60*, 2763.
- (26) Pascher, I.; Pearson, R. H. *Nature* **1979**, *281*, 499.
- (27) Seddon, J. M. In *Phospholipids Handbook*; Cevc, G., Ed.; Marcel Dekker: New York, 1993; p 909.
- (28) Roberts, M. F.; Bothner-By, A. A.; Dennis, E. A. *Biochemistry* **1978**, *17*, 935.
- (29) Matsui, Y.; Mochida, K. *Bull. Chem. Soc. Jpn.* **1979**, *52*, 2808.
- (30) Spencer, J. N.; DeGarmo, J.; Paul, I. M.; He, Q.; Ke, Z.; Yoder, C. H.; Chen, S.; Mihalick, J. E. *J. Solution Chem.* **1995**, *24*, 601.
- (31) Andini, S.; Castronuovo, G.; Elia, V.; Gallotta, E. *Carbohydr. Res.* **1991**, *217*, 87.
- (32) Tominaga, T.; Hachisu, D.; Kamado, M. *Langmuir* **1994**, *10*, 4676.
- (33) Funasaki, N.; Uemura, Y.; Hada, S.; Neya, S. *J. Phys. Chem.* **1996**, *100*, 16298.